第 25 卷第 1 期 无 机 化 学 学 报 Vol.25 No.1
2009 年 1 月 CHINESE JOURNAL OF INORGANIC CHEMISTRY 87~91

离子对间电荷转移配合物:阴离子…π 作用及近红外吸收

刘建兰[1] 姚丙乾[1] 任小明*,[1,2] 沈临江[3] 孟庆金[2]
([1]南京工业大学应用化学系,南京 210009)
([2]南京大学配位化学研究所,配位化学国家重点实验室,南京 210093)
([3]南京工业大学应用物理学系,南京 210009)

摘要:合成并表征了一种离子对配合物 **1**,$[Cl_2Bz\text{-}1\text{-}Apy]_2[Ni(mnt)_2]$,其中,$Cl_2Bz\text{-}1\text{-}Apy$ 为(*E*)-1-(3,4-二氯苯亚甲基氨基)吡啶一价阳离子,mnt 是马来二睛基二硫烯二价阴离子。在配合物 **1** 的晶体中,阴离子和阳离子中吡啶环之间存在阴离子…π 相互作用。DFT 电荷密度分布分析表明,阴离子…π 相互作用主要源自离子对间的 Coulomb 吸引力。在固体和乙腈溶液电子吸收光谱近红外区,配合物 **1** 都有一个宽的弱吸收带,该吸收带可归属为二价阴离子$[Ni(mnt)_2]^{2-}$内的 *d-d* 电子跃迁和阴阳离子对间的电荷转移跃迁。

关键词:离子对;阴离子…π 相互作用;电荷转移;晶体结构;DFT 计算
中图分类号:O614.81+3 **文献标识码**:A **文章编号**:1001-4861(2009)01-0087-05

Observation of Anion…π Interaction and Near IR Absorption in an Ion-Pair Charge Transfer Complex

LIU Jian-Lan[1] YAO Bing-Qian[1] REN Xiao-Ming*,[1,2] SHEN Lin-Jiang[3] MENG Qing-Jin[2]
([1]*Department of Applied Chemistry, College of Science, Nanjing University of Technology, Nanjing* 210009)
([2]*Coordination Chemistry Institute & State Key Lab, Nanjing University, Nanjing* 210093)
([3]*Department of Applied Physics, College of Science, Nanjing University of Technology, Nanjing* 210009)

Abstract: An ion-pair complex, $[Cl_2Bz\text{-}1\text{-}Apy]_2[Ni(mnt)_2]$ ($Cl_2Bz\text{-}1\text{-}Apy^+$=(E)-1-(3,4-di-chlorobenzylideneamino) pyridinium and mnt^{2-}=maleonitriledithiolate), was synthesized and characterized. The anion…π interaction is observed. Based on the DFT analysis, the intermolecular interaction can be attributed to Coulomb interaction. The UV-Vis-NIR spectra of the ion-pair complex in solid state and acetonitrile solution exhibit a weak absorption band in the near IR region, which might originate from the *d-d* transition in $[Ni(mnt)_2]^{2-}$ dianion or IPCT (ion-pair charge transfer) transition between the cation and anion. CCDC: 692922.

Key words: ion-pair; anion…π interaction; charge transfer; crystal structure; DFT calculation

Compounds with an intense near-IR absorption are currently attracting widespread interest for their use in the conversion of sunlight to electricity[1~3] and laser printers[4,5]. It is well known that the donor-acceptor type salt could give rise to a charge transfer (CT) transition band in its electronic absorption spectrum, with band position depending on the energy gap between acceptor LUMO and donor HOMO. Consequently, the spectral property for such a charge transfer transition band is tunable via systematic modification of the acceptor/donor molecular structure[6]. The bis (1,2-dithiolato) metal complexes show intense near-IR absorbance[7], and the origin of this transition may be discussed under two headings: (1) the HOMO and LUMO are delocalized

收稿日期:2008-08-05。收修改稿日期:2008-09-05。
国家自然科学基金资助项目(No.10774076,20771056,20490218);江苏省自然科学基金(No.BK2007184)。
*通讯联系人。E-mail:xmren@njut.edu.cn
第一作者:刘建兰,男,42 岁,博士;研究方向:功能性配合物。

over two dithiolate ligands, and electronic transition between these orbitals gives rise to a strong absorption in the near-IR region. Donor substituents in the parent dithiolate raise the energy level of HOMO more than that of LUMO, resulting in a shift of the near-IR absorbance to lower frequencies; (2) the electronic transition from the HOMO of the bis (1,2-dithiolato) metal anion to the LUMO of the cation gives rise to an intense ion-pair charge transfer (IPCT) band in the near-IR region[7]. Therefore, modifying the molecular structure of the cation provides a useful strategy for the fine-tuning of IPCT band.

Herein we present synthesis, crystal structure, UV-Vis-NIR spectrum and DFT analysis for a new IPCT complex $[Cl_2Bz\text{-}1\text{-}Apy]_2[Ni(mnt)_2]$ ($Cl_2Bz\text{-}1\text{-}Apy^+$= (*E*)-1-(3,4-dichlorobenzylideneamino)pyridinium and mnt^{2-}=maleonitriledithiolate).

1 Experimental section

1.1 Chemicals and reagents

All reagents and chemicals were purchased from commercial sources and used without further purification.

1.2 Physical measurements

Elemental analyses were performed with an Elementar Vario EL Ⅲ analytic instrument. IR spectra were recorded on a Bruker Vector 22 Fourier Transform Infrared Spectrometer (170SX) (KBr disc). ^1H NMR spectra were carried out with an AVANCE AV-300 NMR spectrometer and the chemical shifts were measured relative to the TMS signal. UV-Vis absorption spectra in the solid state and solution were taken using a Cary 5000 UV-Vis-NIR and a Lambda 35 UV/VIS Spectrophotometer, respectively.

1.3 Preparations for 1

Materials. Disodium maleonitriledithiolate (Na_2mnt)[8] and 1-aminopyridinium iodide ([1-APy]I)[9] were synthesized following the respectively published procedures. $[Cl_2Bz\text{-}1\text{-}Apy]I$ was prepared employing a similar procedure described in the literatures[10,11].

$[Cl_2Bz\text{-}1\text{-}Apy]_2[Ni(mnt)_2]$ (1). Na_2mnt (458 mg, 2.46 mmol) and $NiCl_26H_2O$ (230 mg, 0.96 mmol) were mixed under stirring in MeOH (30 mL) at room temperature. Subsequently, a solution of $[Cl_2Bz\text{-}1\text{-}Apy]I$ (948 mg, 2.5 mmol) in MeOH (15 mL) was added to the mixture, and the brown precipitate that was immediately formed was filtered off, and washed with MeOH. The crude product was recrystallized in acetonitrile (20 mL) to give dark-brown crystals. Yield: 81%. Anal. Calc. for $C_{32}H_{18}N_8Cl_4S_4Ni$ (%): C, 45.58; H, 2.15; N, 13.29. Found (%): C, 45.52; H, 2.11; N, 13.24. IR spectrum (KBr, cm^{-1}): 2 194.6(s) for $\nu_{C\equiv N}$ and 1 481.1(s) for $\nu_{C=C}$ of mnt^{2-}, and 1619. 9(m) for $\nu_{C=N}$ of Schiff base.

The single crystals suitable for X-ray analysis were obtained by diffusing diethyl ether into the solution of **1** in acetone for 7 days.

1.4 X-ray crystal structure analysis

The diffraction data for **1** were collected at 296 K with graphite-monochromatized Mo $K\alpha$ (λ=0.071 073 nm) on a Bruker-SMART APEX CCD diffractometer. Data reductions and absorption corrections were performed with the SAINT and SADABS software packages[12], respectively. Structure was solved by the direct method and refined by the full-matrix least-squares procedure on F^2 using SHELX-97 program[13]. All non-hydrogen atoms were refined anisotropically, and the hydrogen atoms were introduced at calculated positions. The crystallographic details about data collection and structure refinement are summarized in Table 1.

CCDC: 692922.

Table 1 Crystal and structural refinement data of 1

Chemical formula	$C_{32}H_{18}Cl_4N_8NiS_4$	Density / ($g\cdot cm^{-3}$)	1.621
Formula weight	843.29	Abs coeff. / mm^{-1}	1.151
Temperature / K	296(2)	*F*(000)	426
Crystal system	Triclinic	Data collect θ range / (°)	2.12~24.99
Space group	$P\bar{1}$	Reflection collected	4 345

Continued Table 1

a / nm	0.868 6(3)	Indep. refls. (R_{int})	2 994 (0.047 7)
b / nm	1.039 0(4)	Observed reflections	2 489
c / nm	1.090 7(3)	Index range	$-10 \leqslant h \leqslant 10, -7 \leqslant k \leqslant 12, -12 \leqslant l \leqslant 12$
α / (°)	61.56(3)	Data / restraints / parameters	2 994 / 0 / 224
β / (°)	88.314(5)	Goodness-of-fit on F^2	1.048
γ / (°)	86.457(4)	Final R_1 and wR_2 [$I>2\sigma(I)$]	0.035 2, 0.089 6
V / nm^3	0.863 9(5)	Residual peak and hole / (e·nm^{-3})	542 and −420
Z	1		

$R_1=\sum(||F_o|-|F_c||)/\sum|F_o|$, $wR_2=\sum w(|F_o|^2-|F_c|^2)^2/\sum w(|F_o|^2)^2]^{1/2}$.

1.5 DFT calculation details

All calculations for geometric optimization were carried out with the Gaussian98 program[14] by restricted density functional theory (DFT). Becke′s three-parameter functional[15] with Lee-Yang-Parr′s correlation functional[16,17] (B3LYP) and 6-31G(d,p)[18,19] basis set were employed for the cation and B3LYP with 6-31G(d, p) basis set for C, N and S atoms, LANL2DZ[20,21] basis set for Ni atom were employed for the $[Ni(mnt)_2]^{2-}$ anion.

2 Results and discussion

2.1 Description of crystal structure

As shown in Fig.1a, an asymmetric unit of complex **1** consists of one $[Cl_2Bz\text{-}1\text{-}Apy]^+$ cation and one half $[Ni(mnt)_2]^{2-}$ anion. The cation is almost planar and the interplanar angle between the pyridine and benzene rings is 4.5(2)°. The $[Ni(mnt)_2]^{2-}$ anion also exhibits a planar molecular geometry, in which Ni^{2+} ion occupies a crystallographic inversion center, the Ni-S bond lengths are 0.217 72(9) and 0.217 72(10) nm, and the S-Ni-S bite angle is 91.80(4)°, these bond parameters are comparable to the reported values[22]; of particular note is that the anion is flanked by two cations which are related to each other via a crystallographic inversion centre to form a sandwich-type structure (Fig.1b and 1c), in such a sandwich there probably exists anion…π interaction between the pyridine ring and $[Ni(mnt)_2]^{2-}$ anion [the dihedral angle between the mean planes of $[Ni(mnt)_2]^{2-}$ anion, defined by four coordinated S-atoms, and pyridine ring is 11.26(13)°; and the shorter interatomic contacts are found as 0.350 5(3) nm of C(8)…S(1) ($1-x$, $-y$, $1-z$), 0.354 1(3) nm of C(9)…Ni(1), 0.361 8(2) nm of N(3)…Ni(1) and 0.360 8(3) nm of N(4)…S(1), respectively]. Additionally, there exist S…Cl and weak H-bonding interactions between the neighboring anions and cations, such intermolecular interactions lead to the neighboring anions and cations forming a molecular sheet (Fig.2), which is parallel to

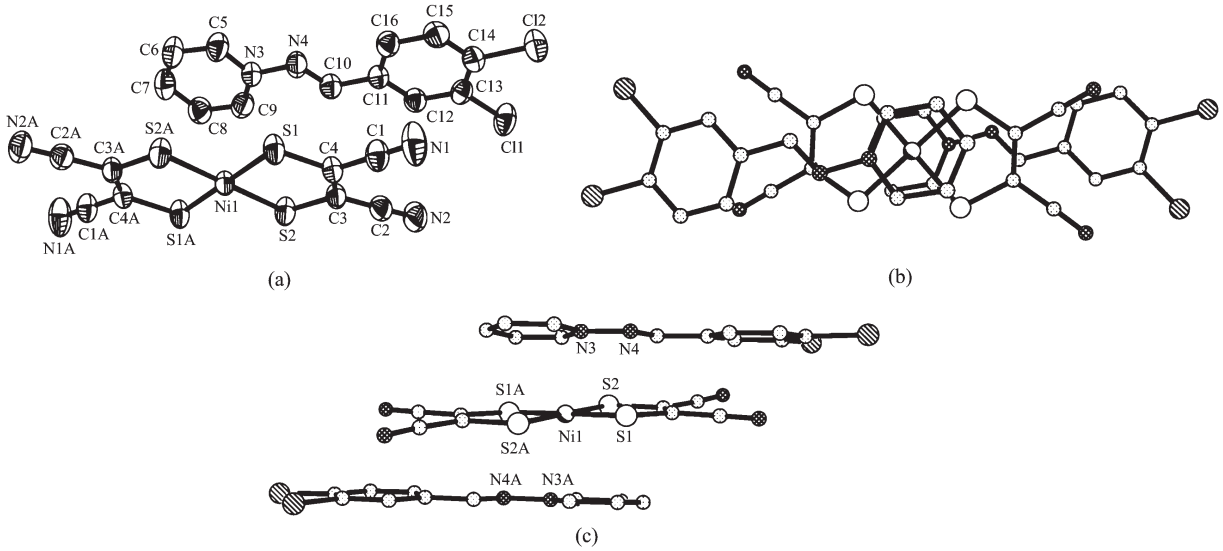

Fig.1 (a) ORTEP view of **1** with thermal ellipsoids at the 50% probability level and H-atoms omitted for clarity; (b) top and (c) side views showing a sandwich-type structure with anion…π interactions

the crystallographic (111) plane. The neighboring molecular sheets further develop into three-dimensional supramolecular network via anion···π interactions.

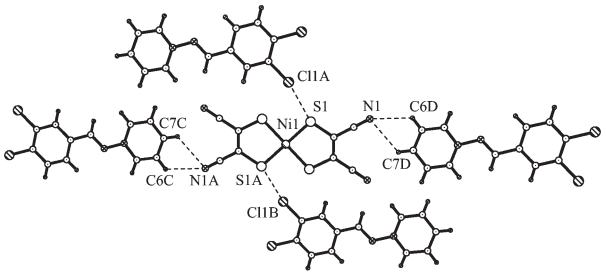

$d_{S(1)\cdots Cl(1A)}$=0.342 2(1) nm, the symmetric code A=x, −1+y, z; H-bonding geometric parameters: $d_{N(1)\cdots H(6DA)}$=0.260 0 nm, $d_{N(1)\cdots C(6D)}$=0.323 7(4) nm, N(1)···H(6DA)–C(6D)=126.11°; $d_{N(1)\cdots H(7DA)}$=0.269 5 nm, $d_{N(1)\cdots C(7D)}$=0.328 1(4) nm, N(1)···H(7DA)–C(7D)=121.74° and the symmetric code D=x, 1+y, −1+z

Fig.2 Molecular sheet formed by anions and cations through intermolecular S···Cl and weak H-bonding interactions

2.2 UV-Vis-NIR spectra

The UV-Vis-NIR spectrum of **1** in the solid state shows the intense absorbance in the UV/visible region (200 ~720 nm) with a shoulder absorption band at around 810 nm and the low energy absorption tail extends up to ca. 1000 nm in the near-IR region (Fig.3a and Table 2). The UV-Vis-NIR spectra of **1**, [Cl_2Bz-1-Apy]I as well as [TBA]$_2$[Ni(mnt)$_2$] in acetonitrile (Fig. 3b and 3c) exhibit characteristics: (1) a series of bands with high molar absorptions (ε >10^4) in the range of 200 ~360 nm which can be assigned to the $\pi \rightarrow \pi^*$ transitions within the cation and anion; (2) the band centered at 473 nm does not appear in the [Cl_2Bz-1-Apy]$^+$ cation, the intensity is independent of the cationic concentration, and this absorption band can be assigned to the transition in [Ni(mnt)$_2$]$^{2-}$[23]; (3) the weak absorption band centered at around 862 nm, which appears in the spectra of [TBA]$_2$[Ni(mnt)$_2$] and [Cl_2Bz-1-Apy]$_2$[Ni(mnt)$_2$] and its absorption intensity depends slightly on the cationic concentration, might originate from the transition in [Ni(mnt)$_2$]$^{2-}$ dianion[23] or IPCT transition between the cation and anion.

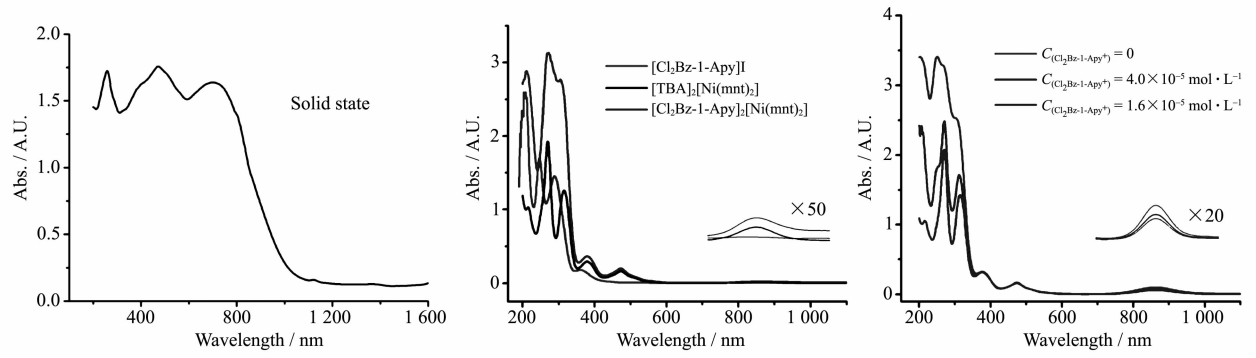

Fig.3 (a) Diffuse reflectance spectrum of 1 in solid state; (b) absorbance spectra of **1** (5.0×10^{-5} mol·L^{-1}), [Cl_2Bz-1-Apy]I (1.0×10^{-4} molL^{-1}) as well as [TBA]$_2$[Ni(mnt)$_2$] (5.0×10^{-5} mol·L^{-1}) in acetonitrile solution; (c) absorbance spectra of [TBA]$_2$[Ni(mnt)$_2$] with different concentration of [Cl_2Bz-1-Apy]I

Table 2 Optical properties of complex 1 (5.0×10^{-5} mol·L^{-1}), [TBA]$_2$[Ni(mnt)$_2$] (5.0×10^{-5} mol·L^{-1}) as well as [Cl_2Bz-1-Apy]I (1.0×10^{-4} mol·L^{-1}) in acetonitrile solution

λ_{max} / nm (ε / (L·mol^{-1}·cm^{-1}))					
[Cl_2Bz-1-Apy]$_2$[Ni(mnt)$_2$]					
211(57 735)	270(62 437)	304(55 409)	379(7 230)	473(3 263)	863(488)
[TBA]$_2$[Ni(mnt)$_2$]					
216(20 650)	270(38 482)	315(25 160)	380(5 794)	473(3 263)	862(291)
[Cl_2Bz-1-Apy]I					
209(25 986)	247(16 977)	289(14 533)	361(1 768)		

2.3 DFT analyses

The anion-π interaction has recently become a challenge in supramolecular chemistry, which is generally found between an electron-deficient π-electron system of aromatic compounds and a simple inorganic anion, and in which case the contributions

from electrostatic interactions and anion induced polarization are energetically favorable [24]. To better understand the anion … π interaction, the geometric optimizations and charge distributions for both anion and cation were respectively performed, and the main theoretical results are summarized below: (1) the stable conformation is the perfect planar molecular geometry for the $[Ni(mnt)_2]^{2-}$ anion, while the non-planar geometry for the cation due to the steric hindrance between two hydrogen atoms which are attached on C(9) and C(10) atoms, respectively (atomic labeling please see Fig.1a); (2) the N(4) and C(10) atoms are coplanar with benzene ring, and the interplanar angle between pyridine and benzene rings is 51.1 (cf. Fig.1a and Fig.4); (3) the sum of charge density is +0.625 72e for the pyridine ring in the $[Cl_2Bz\text{-}1\text{-}Apy]^+$ cation and −0.442 02e for the NiS_4 core in the $[Ni(mnt)_2]^{2-}$ anion. These results imply that the energy barrier between the non-planar and planar conformation is not much higher than the realms of crystal packing forces for the $[Cl_2Bz\text{-}1\text{-}Apy]^+$ cation, and the anion … π interaction is mainly attributed to Coulomb interaction.

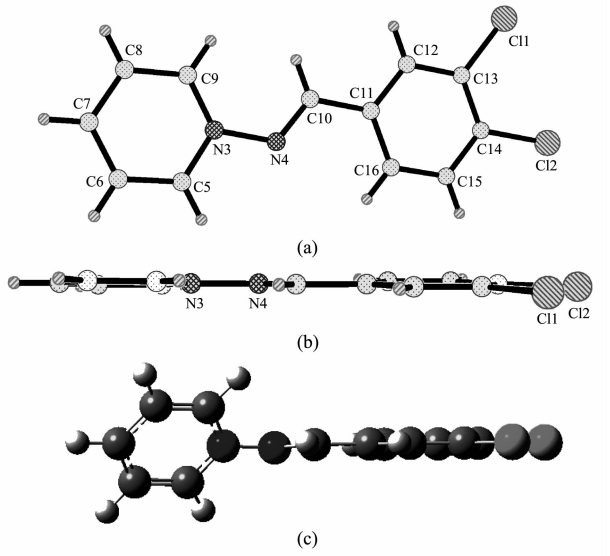

Fig.4 Molecular structure of (*E*)-1-(3,4-dichlorobenzylideneamino)pyridinium (a) top and (b) side views from X-ray crystallography shows planar geometry; (c) from geometric optimization shows non-planar geometry

3 Conclusions

There is a planar anion … π interaction in the ion-pair complex $[Cl_2Bz\text{-}1\text{-}Apy]_2[Ni(mnt)_2]$. Theoretical analysis indicated such intermolecular interaction can be attributed to Coulomb interaction. The UV-Vis-NIR spectra in both solid state and acetonitrile solution exhibit a weak absorption band in the near IR region, which might originate from the transition in $[Ni(mnt)_2]^{2-}$ dianion or IPCT transition between the cation and anion.

References:

[1] Horiuchi T, Miura H, Sumioka K, et al. *J. Am. Chem. Soc.*, **2004**,**126**:12218~12219

[2] Bach U, Lupo D, Comte P, et al. *Nature*, **1998**,**395**:583~585

[3] Cid J J, Yum J H, Jang S R, et al. *Angew. Chem. Int. Ed.*, **2007**,**46**:8358~8362

[4] Herman Z S, Kirchner R F, Loew G H, et al. *Inorg. Chem.*, **1982**,**21**:46~56

[5] Endo A, Matsumoto S, Mizuguchi J. *J. Phys. Chem. A*, **1999**, **103**:8193~8199

[6] Güsten H, Klasinc L. *J. Phys. Chem.*, **1972**,**76**:2452~2454

[7] Madhu V, Das S K. *Polyhedron*, **2004**,**23**:1235~1242

[8] Davison A, Holm H R. *Inorg. Synth.*, **1967**,**10**:8~26

[9] Richard G, Alwin M. *Chem. Ber.*, **1959**,**92**:2521~2531

[10]Kurkutova E N, Levina O I, Sheynkman A K, et al. *Zh. Strukt. Khin.*, **1976**,**17**:881~885

[11]Tian Z F, Ren X M, Li Y Z, et al. *Inog. Chem.*, **2007**,**46**:8102~8104

[12]*Software Packages SMART and SAINT, Siemens Analytical X-ray Instrument Inc.*, Madison, WI, **1996**.

[13]Sheldrick G M. *SHELX*-97, *Program for the Solution and the Refinement of Crystal Structure*, University of Göttingen, Germany, **1997**.

[14]Frisch M J, Trucks G W, Schlegel H B, et al. *Gaussian* 98, *Revision A*.11, Gaussian, Inc., Pittsburgh PA, **2001**.

[15]Becke A D. *J. Chem. Phys.*, **1993**,**98**:5648~5653

[16]Lee C, Yang W, Parr R G. *Phys. Rev. B*, **1988**,**37**:785~789

[17]Miehlich B, Savin A, Stoll H, et al. *Chem. Phys. Lett.*, **1989**, **157**:200~206

[18]Ditchfield R, Hehre W J, Pople J A. *J. Chem. Phys.*, **1971**,**54**: 724~728

[19]Gordon M S. *Chem. Phys. Lett.*, **1980**,**76**:163~168

[20]Wadt W R, Hay P J. *J. Chem. Phys.*, **1985**,**82**:284~298

[21]Hay P J, Wadt W R. *J. Chem. Phys.*, **1985**,**82**:299~310

[22]Ren X M, Duan C Y, Zhu H Z, et al. *Trans. Met. Chem.*, **2001**,**26**:295~299

[23]Shupacke S I, Billig E, Clark R J H, et al. *J. Am. Chem. Soc.*, **1964**,**86**:4594~4602

[24]Berryman O B, Bryantsev V S, Stay D P, et al. *J. Am. Chem. Soc.*, **2007**,**129**:48~58